

MEASUREMENT OF THE INTENSITY-DEPENDENT REFRACTIVE INDEX USING COMPLETE SPATIO-TEMPORAL PULSE CHARACTERIZATION

GIOVANNI PIREDDA*, CHRISTOPHE DORRER†, ELLEN M. KOSIK WILLIAMS‡,
IAN A. WALMSLEY§ and ROBERT W. BOYD

*The Institute of Optics, University of Rochester
Rochester, NY 14627, USA*

**piredda@optics.rochester.edu*

Received 20 May 2004

We use complete spatio-temporal characterization of an ultrashort pulse to study self-phase modulation and other propagation effects in a sample of SF59 optical glass. The goal of this work is to perform accurate experimental measurements of the optical parameters of material samples. From the measured dependence of the self-induced phase shift on the transverse coordinate, we deduce a value of the coefficient n_2 of the intensity-dependent refractive index that is in good agreement with previous measurements. We also observe that the spectrum of the transmitted pulse can be explained only approximately in terms of the solution to the nonlinear Schrödinger equation.

Keywords: Full-field characterization; ultrashort pulses; nonlinear refractive index; glasses.

1. Introduction

The use of ultrashort pulses to measure nonlinear optical constants is attractive: these techniques make it possible to isolate the contribution of the ultrafast component of the nonlinearity under study; furthermore high intensities can be reached at low average power levels, making it easier to control experimental conditions such as the temperature rise of the sample.

Two issues merit consideration. One is that in order to interpret the results of the measurements, and thereby to obtain values of the optical constants from raw data, it is necessary to consider in a careful way the propagation of the optical

†Now at Bell Laboratories — Lucent Technologies, 101 Crawfords Corner Road, Holmdel, NJ 07733.

‡Now at Sullivan Park, Corning Incorporated, Corning, NY 14831, USA.

§Now at Clarendon Laboratory, University of Oxford, Parks Road, Oxford OX1 3PU, UK.

pulses through the test material. The parameters that describe ultrashort pulses, such as temporal duration, chirp, spectrum, and more generally the details of their time dependence, can change so much during the propagation of the pulse through the material that they cannot be approximated by their values at the input or by an average. The second issue is that propagation of ultrashort pulses through a medium with nonlinearities involves two effects: spatial phase modulation and temporal phase modulation. Most techniques for the measurement of n_2 involve only one of these effects. For example the often-used Z-scan technique¹ extracts n_2 from a single measurement that involves only spatial phase modulation, whereas other methods such as spectrally-resolved two-beam coupling² use only temporal data. However, a complete characterization of the spatial and temporal variation of the field allows a simultaneous determination of n_2 from both spatial and temporal phase modulation at the same time, making it possible to use one effect as a check for the other.

Steps toward complete characterization of optical pulses have been made in the works by Gallmann and co-authors³ and Diddams and co-authors.⁴ In both of these works spatially-resolved measurements on ultrashort pulses were performed by an array of independent measurements; as a consequence of the fact that measurements at different positions in space are not related to each other the techniques used in these works do not allow the measurement of the spatial dependence of the phase. In this paper we implement spacetime spectral phase interferometry for direct electric field reconstruction (spacetime SPIDER)^{5,6} to characterize the propagation of an ultrashort pulse through a piece of SF59 glass; with this experimental technique we are able to observe at the same time the spatial and temporal effects of self-phase modulation. We simulate the propagation of the pulse through the glass using the nonlinear Schrödinger equation and by concentrating on transverse phase variations we extract a value of n_2 consistent with that of previous measurements.⁷⁻⁹ However, we observe that the spectrum of the pulse transmitted through the glass cannot be precisely matched by the solution to the nonlinear Schrödinger equation. This disagreement is not resolved even when we take into account additional effects such as the exact dispersion relation for the material and other plausible nonlinear processes, such as higher-order (n_4) nonlinearities, the dependence of the group velocity on intensity, and Raman scattering. We feel that once these problems are solved this technique can be usefully exploited for the measurement of material properties using ultrashort pulses.

2. Experiment

The experimental technique consists of letting an ultrashort, high-intensity pulse pass through a sample of the glass and characterizing it in a complete way before and after its passage through the sample (Fig. 1). The characterization is performed with a method, spacetime SPIDER,^{5,6} that is a generalization of the SPIDER technique.¹⁰ The pulse becomes modified in passing through the glass sample, and

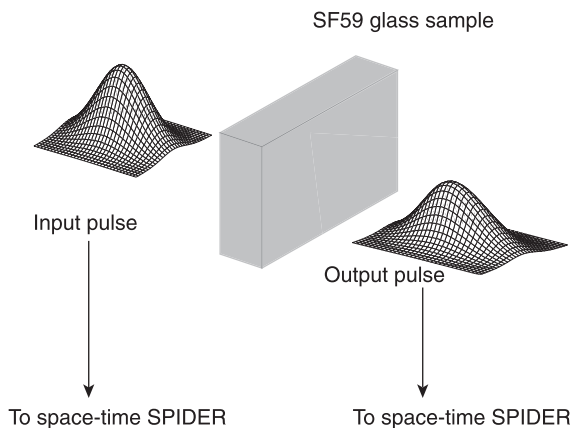


Fig. 1. An ultrashort high-energy pulse is completely characterized before and after its passage through a SF59 glass sample.

it is possible to calculate the parameters of the material in terms of the measured changes in the pulse.

Conventional SPIDER obtains the complete characterization of the electric field $\tilde{E}(\omega)$ by measuring the phase $\phi(\omega)$ of its analytic signal $E(\omega)$. A separate measurement of the spectral intensity completes the data. The phase is measured by spectral shearing. Two replicas of the pulse, separated by a relative delay of τ , generated for example with a Michelson interferometer, are upconverted in a nonlinear crystal with a highly chirped pulse; the chirp must be high enough so that the chirped pulse looks like a monochromatic wave on the timescale of the pulse to be measured. The spectral shear is generated because the two replicas interact each with a different portion of the chirped pulse (with respective instantaneous frequencies Ω and $\Omega + \Delta\omega$) and are upconverted to two slightly different frequencies. The two upconverted replicas, $E_1(\omega) = E(\omega - \Omega)$ and $E_2(\omega) = E(\omega - \Omega - \Delta\omega) \exp(i\omega\tau)$, are examined in a spectrometer. The measured spectrum, $|E_1(\omega) + E_2(\omega)|^2 = |E(\omega - \Omega)|^2 + |E(\omega - \Omega - \Delta\omega)|^2 + 2|E(\omega - \Omega)||E(\omega - \Omega - \Delta\omega)| \cos(\phi(\omega - \Omega) - \phi(\omega - \Omega - \Delta\omega) - \omega\tau)$, contains in the interference term the difference between the phase of the pulse at neighboring frequencies. For small enough $\Delta\omega$ the phase difference approximates the derivative $d\phi/d\omega$ and the phase at every frequency can be reconstructed.

Spacetime SPIDER is illustrated in Figs. 2 and 3, which are adapted from Ref. 6. In this case the phase ϕ must be resolved both spatially and spectrally: in addition to the spectral gradient $\partial\phi(x, \omega)/\partial\omega$ it is necessary to obtain the spatial gradient $\partial\phi(x, \omega)/\partial x$. These gradients are obtained by applying separately spatial and spectral shears to the two replicas of the pulse and analyzing the replicas in an imaging spectrometer.

The spectral shearing (Fig. 2(a)) is realized with the SPIDER technique. In this case the nonlinear interaction takes place at the Fourier plane of a double-Fourier-transform setup. After the second lens the upconverted replicas are detected in an

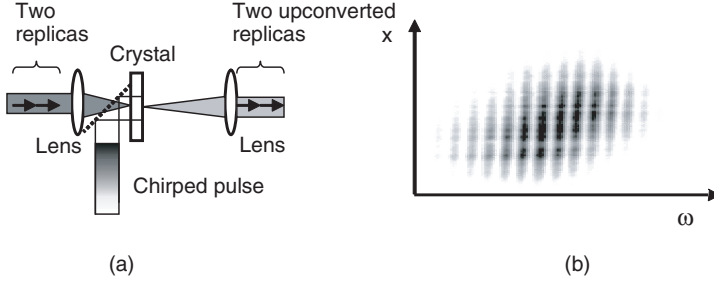


Fig. 2. (a) Generation of a spectral shear with the SPIDER technique, and (b) spatially-resolved spectral interferogram.

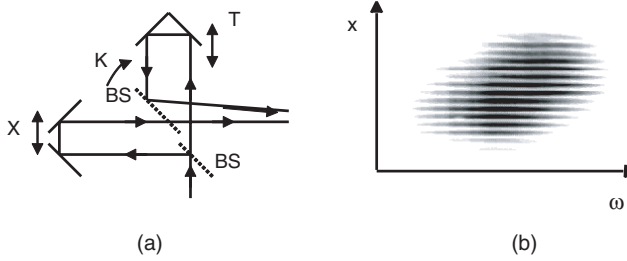


Fig. 3. (a) Generation of a spatial shear with a Michelson interferometer, and (b) spectrally-resolved spatial interferogram.

imaging spectrometer, thus obtaining a SPIDER interferogram for every transverse location x in the pulse (Fig. 2(b)). This setup preserves the spatial information in the pulse and allows us to extract the spectral gradient $\partial\phi/\partial\omega$ of the phase of the pulse as a function of both ω and x .

The spatial shearing is realized by imaging the pulse on the slit of the imaging spectrometer after passing it through a Michelson interferometer (Fig. 3(a)). The interferometer provides independent control of the shear X , tilt K and delay T of the replicas. The detected signal (Fig. 3(a)), shown for the case of zero delay, is a spectrally-resolved spatial shearing interferogram. The spatial gradient $\partial\phi/\partial x$ of the phase of the pulse can be extracted from this interferogram as a function of ω and x .

The phase of the pulse can be reconstructed from the knowledge of the two independent gradients.

The complete knowledge of the optical field provides more data than is necessary to calculate n_2 . We find that, for our experimental conditions, it is convenient to consider the transverse phase variation of the pulse at a fixed local time of the pulse (e.g. at the peak of the pulse). We show that among the various parameters that could be used to measure n_2 this is a convenient one because it is easy to establish experimental conditions where diffraction is negligible and thus the phase differences along the transverse direction depend on n_2 in a straightforward manner.

2.1. Experimental data

Our data describe a pulse produced by a Ti:Sapphire laser and amplified by a regenerative amplifier operating at a 1 kHz repetition rate; the pulse has travelled through a 1.25 cm thick sample of SF59 glass. The center wavelength of the pulse is 819 nm. The pulse has an energy of $21 \mu\text{J}$, a transverse size (FWHM) of 0.2 cm and a duration (FWHM) of 63 fs before entering the sample. At the exit the transverse size is unchanged; the duration is 200 fs. The pulse shows self-phase modulation at the exit of the sample (see input and output intensity and phase respectively in Figs. 4 and 5).

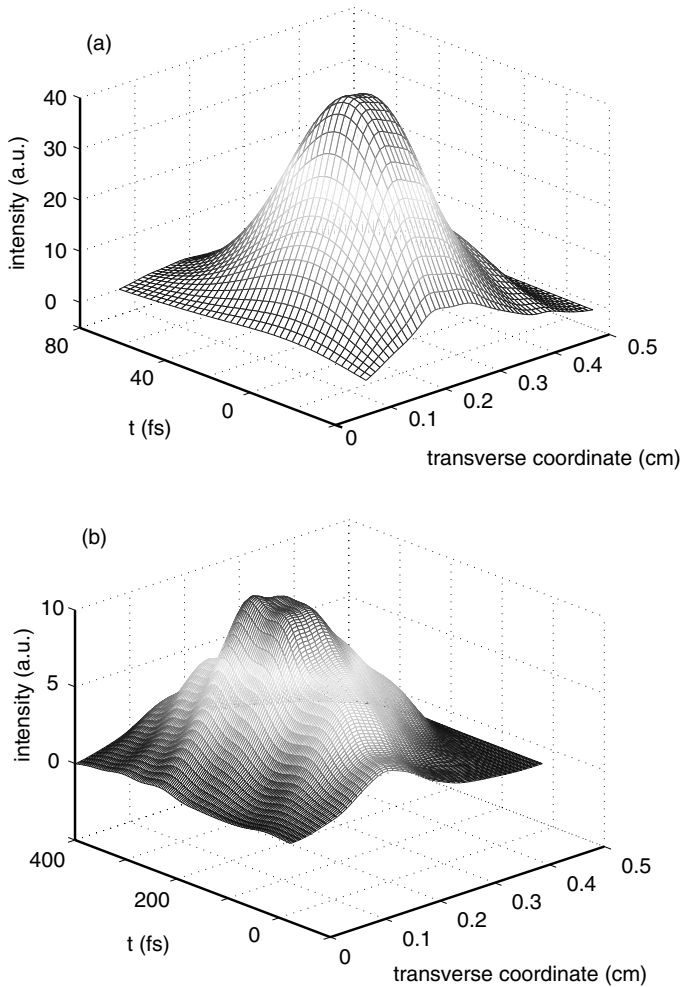


Fig. 4. Variation of the pulse intensity with time and transverse coordinate at (a) the input, and (b) the output, of the SF59 glass sample as measured by spacetime SPIDER.

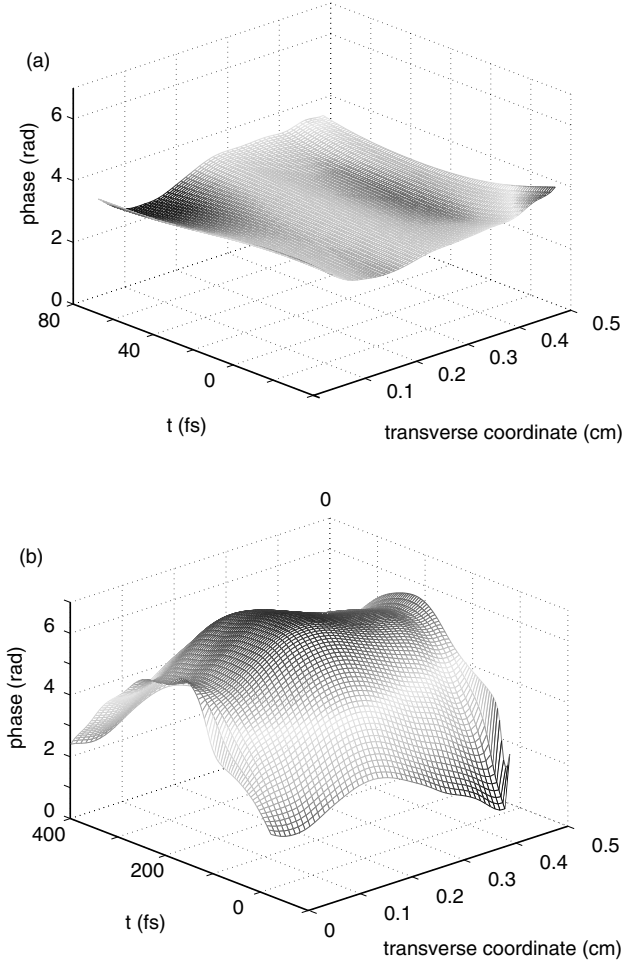


Fig. 5. Variation of the pulse phase with time and transverse coordinate at (a) the input, and (b) the output, of the SF59 glass sample as measured by spacetime SPIDER.

3. Analysis of the Data and Calculation of n_2

The optical pulse that travels through the glass is subject to modification through three main processes: diffraction, dispersion, and the dependence of the refractive index on the intensity. The importance of each of these can be estimated by evaluating the phase shift that it imparts on the pulse. These phases are

$$\Delta\phi_{\text{diffr}} \approx \frac{1}{4\pi} \frac{\lambda z}{\delta^2} \approx 10^{-3} \text{ rad} \quad (1)$$

$$\Delta\phi_{\text{disp}} \approx \frac{1}{2} \frac{\beta_2 z}{\tau^2} \approx 0.5 \text{ rad} \quad (2)$$

$$\Delta\phi_{\text{NL}} \approx \frac{2\pi}{\lambda} I_0 n_2 z \approx 1.5 \text{ rad} \quad (3)$$

for diffraction, dispersion and nonlinearity, respectively. Here λ is the central wavelength of the pulse, δ the transverse size, τ the duration; I_0 , the peak intensity, for this pulse is equal to $5.5 \times 10^9 \text{ W/cm}^2$ and z is the propagation distance; the second-order dispersion, $\beta_2 = 2820 \text{ fs}^2/\text{cm}$, is calculated from Schott's tables¹¹ and we use an estimate of $n_2 \approx 5 \times 10^{-15}$ for the intensity-dependent refractive index, based on previous measurements.⁷⁻⁹

The dispersive and nonlinear phases are comparable and the diffractive phase is negligible. This last fact is confirmed also by the observation that the spatial FWHM of the pulse does not change during propagation; the Rayleigh range for this pulse is in the order of 10 m.

The pulse, therefore, almost does not diffract, and we can consider the propagation of a section of the pulse taken along the time axis at a particular location at the transverse direction to be independent of all the other parts of the pulse. It follows that the phase differences between two points that are at the temporal peak of the pulse but at two different locations in space depend in a straightforward way on the intensity as

$$\phi(z, x) = \frac{2\pi}{\lambda} n_2 \int_0^z I(z', x) dz' \quad (4)$$

where $I(z', x)$ is the intensity at a particular position z' along the propagation axis and x across the transverse profile of the pulse.

The intensity variation caused by propagation depends both on the group velocity dispersion and on the nonlinearity, and this fact makes it necessary to calculate the pulse propagation using a numerical method.

We next describe the method that we have followed for extracting a value of n_2 from the data. The idea is to simulate the propagation of the pulse using a computer program for solving the (2 + 1)-D nonlinear Schrödinger equation. The nonlinear Schrödinger equation^{12,13} includes two parameters, one of which, the group velocity dispersion, is known, while the other, the intensity-dependent refractive index, is the one we want to determine. We adjust the intensity-dependent refractive index in our computer code until we reach the best possible least-squares fit between the calculated transverse phase of the output pulse and the observed one; the value of n_2 that yields the best agreement is our inferred n_2 .

Since the phase that we measure is defined within an arbitrary constant, we choose this constant so that the calculated and observed phases coincide at the peak of the pulses. Moreover we weight our least-squares fit with the pulse intensity because the experimental value of the phase is more precise where the intensity is higher.

In order to solve the nonlinear Schrödinger equation we use a Fourier split-step method.¹² We discretize the pulse on a 512×512 grid with a temporal step of 2.9 fs and a transverse step of $23 \mu\text{m}$, which satisfy amply the requirements of the Shannon sampling theorem. We include nonlinear absorption in the propagation

equation. The imaginary part of the intensity-dependent refractive index, measured with the Z-scan technique,¹ is $\text{Im}\{n_2\} = 10 \times 10^{-16} \text{ cm}^2/\text{W}$.

After performing these calculations we find that the value of the real part of n_2 that allows us to best reproduce the experimental data is $\text{Re}\{n_2\} = 65 \times 10^{-16} \text{ cm}^2/\text{W}$; this value is in good agreement with other published measurements.⁷⁻⁹ The error associated with this measurement can be estimated as $\pm 10 \times 10^{-16} \text{ cm}^2/\text{W}$. The comparison of the calculated and measured phases with this value of n_2 is shown in Fig. 6. The agreement with the experimental data is extremely good for the phase and acceptable for the intensity.

We possess more data than the ones that we have considered so far; in principle we have all of the information that can be extracted from both Z-scan and spectrally-resolved two-beam coupling. This fact prompts us to cross-check our simulations; if the model we are using takes into account all of the important physical effects, then the choice of parameters that allows us to reproduce a part of the data should also reproduce all of the other parts. We therefore look at the temporal and spectral intensity of the simulated output pulse and we compare them to the experimental data. The comparison is reported in Fig. 7 for the temporal intensity and Fig. 8 for the spectral intensity. We see that the agreement between the simulated and observed temporal intensities is good, but the simulated output spectrum is significantly different from the experimentally-observed one. This disagreement between the simulated and observed fields suggests that something is not correct in our model. We consider several possibilities in turn.

One possibility is that approximating the dispersion relation with a parabola is simply not accurate enough. In this regard we first note that we have low intensity data, for which nonlinear effects can be completely ruled out, and that these data

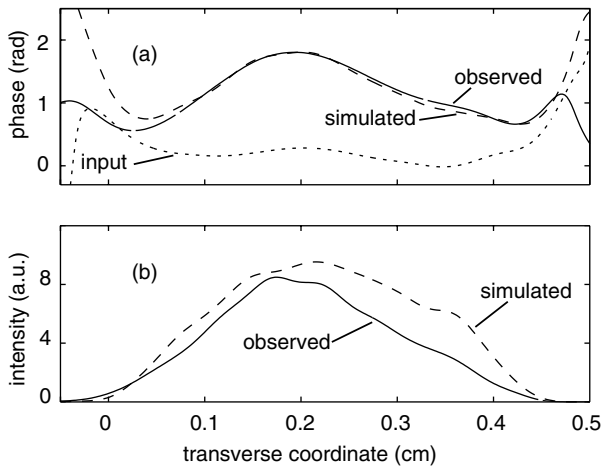


Fig. 6. (a) Input and output transverse phase variations, and (b) output intensity variations.

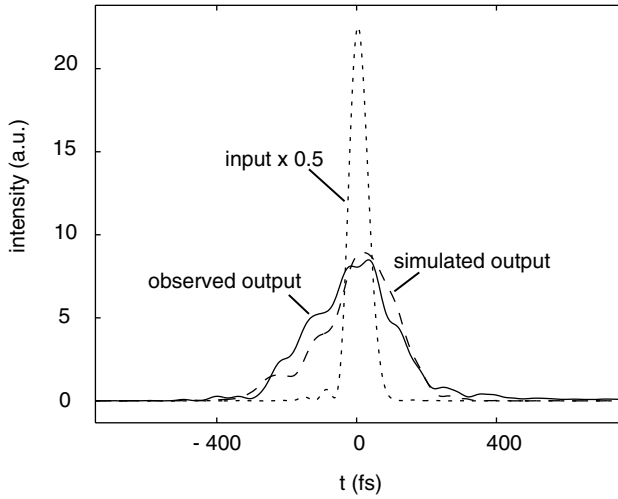


Fig. 7. Variation of the pulse temporal intensity with time as measured at the input and output of the material.

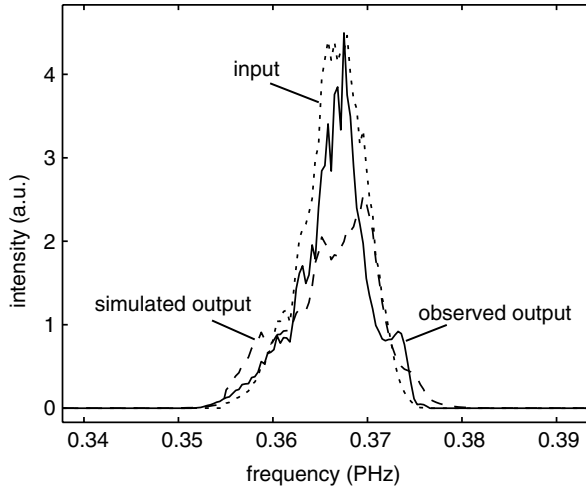


Fig. 8. Variation of the pulse spectral intensity with time as measured at the input and output of the material.

confirm that a GVD parameter of $2820 \text{ fs}^2/\text{cm}$ reproduces correctly the pulse duration after it travels through our sample. In order to test this hypothesis further we substituted into our code the exact dispersion relation, as calculated from Schott's tables,¹¹ for the approximating parabola. The simulations that we performed in this situation gave no discernible difference from the ones in which we used the GVD approximation.

A second possibility is that the slowly varying envelope approximation that one uses in the derivation of the nonlinear Schrödinger equation is not adequate for this pulse. In order to obtain an equation valid for pulses for which the slowly varying envelope approximation does not hold, we added to the nonlinear Schrödinger equation a term that describes the dependence of the group velocity on intensity and is responsible for the formation of optical shocks.^{12,13} Again, there is no effect on the result of the simulation.

The third possibility is that we are not including some physical effect that is actually important. While one can never test all possible additional effects, we have examined a few significant possibilities.

We checked that the inclusion of a higher-order nonlinearity does not modify the results. In particular we considered the possible presence of a dependence of the refractive index on the square of the intensity of light; that is, in the current notation, we looked for n_4 effects. After performing our simulations, using the transverse phase as we did for our determination of n_2 , we did not find any justification for choosing an n_4 value different from 0. In particular inserting n_4 in the simulations does not make the agreement of the transverse phases better and it actually increases the differences between the observed and simulated spectra. We moreover included the effect of stimulated Raman scattering.¹² The retarded nonlinear response has been recently studied with two-beam coupling methods.^{14,15} We found, using for the Raman response function parameters that are valid for fused silica,¹⁶ that the inclusion of the Raman response does not improve the agreement between the theory and the data. No measurements of the Raman response function of SF59 is available in the literature. Finally we did not include the possible

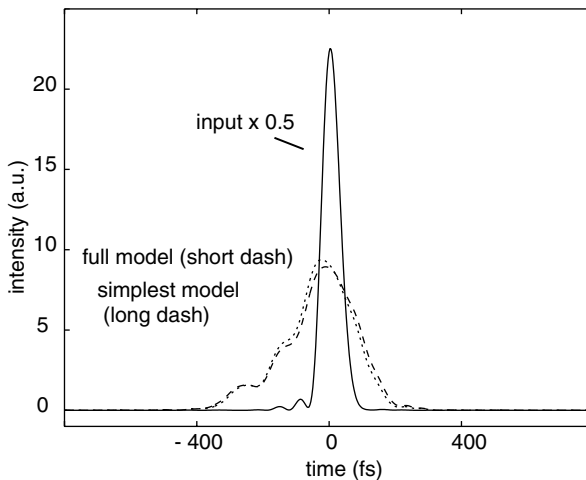


Fig. 9. Comparison of the simulated output temporal intensities obtained with the nonlinear Schrödinger equation (long dash) and with additional terms (short dash). The simulated graphs for the two different cases almost superpose.

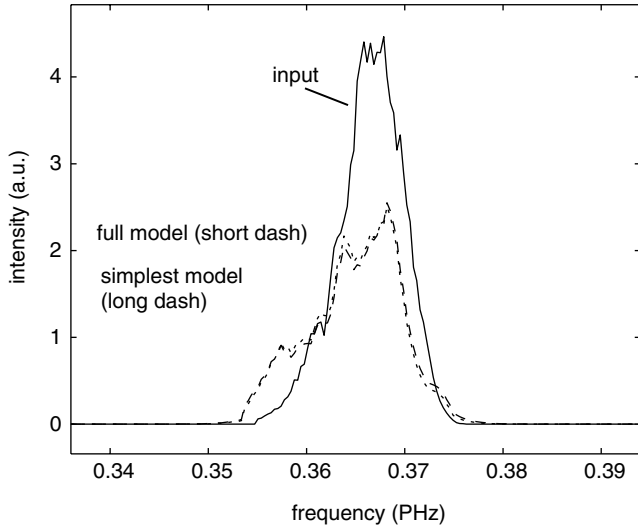


Fig. 10. Comparison of the simulated output spectral intensities obtained with the nonlinear Schrödinger equation (long dash) and with additional terms (short dash). The two simulated graphs for the two different cases almost superpose.

effects of dispersion of n_2 because these effects enter the propagation equation at first order as a correction to the intensity-dependent group velocity term.¹³

Our work with refinements of the nonlinear Schrödinger equation is illustrated in Figs. 9 and 10. In this simulation we included all of the refinements and effects we have mentioned and we compared the output temporal and spectral intensity (indicated in the graph as “full model”) to the ones predicted by the nonlinear Schrödinger equation (indicated in the graph as “simplest model”). As an example we chose a value of n_4 such that its contribution to the phase is approximately 5% of the total nonlinear phase and of opposite sign with respect to the contribution of n_2 . An estimate based on Ref. 17 suggests that in our experiment the contribution of the fifth-order response to the nonlinear phase is smaller than 0.1%; we therefore are exaggerating the importance of this term. The graphs show that corrections to the nonlinear Schrödinger have a negligible effect. Simulations including only one of the additional terms give similar results to the full simulations; in other words in the full simulation there is no significant mutual cancellation of effects.

4. Conclusions

We collected an extensive set of experimental data on the propagation of an ultra-short pulse through a nonlinear glass. We find that the transverse phase of the pulse behaves, to an excellent approximation, as if the pulse were subject just to dispersion and the intensity-dependent refractive index; this model for the propagation is, however, unable to account for other aspects of the data, such as the spectrum of the pulse.

We conclude that a complete set of data about propagation of ultrashort pulses can reveal details of the properties of materials that would be overlooked if one had access only to limited sets of data. We are continuing our experimental and theoretical work to determine under what conditions it is reasonable to use a limited set of data for measurement of nonlinear optical constants with ultrashort pulses.

Acknowledgment

The work performed at the University of Rochester was supported by ONR award N00014-02-1-0797, by DoE award DE-FG02-01ER15156, and by ARO award DAAD19-01-1-0623.

GP and IAW acknowledge useful conversations with Alex Gaeta.

References

1. M. Sheik-Bahae, A. A. Said, T. H. Wei, D. J. Hagan and E. W. Van Stryland, *IEEE J. Quantum Elect.* **26** (1990) 760.
2. I. Kang, T. Krauss and F. Wise, *Opt. Lett.* **22** (1997) 1077.
3. L. Gallmann, G. Steinmeyer, D. H. Sutter, T. Rupp, C. Iaconis, I. A. Walmsley and U. Keller, *Opt. Lett.* **26** (2001) 96.
4. S. A. Diddams, H. K. Eaton, A. A. Zozulya and T. S. Clement, *Technical Digest, Conference on Lasers and Electro-Optics, CLEO 98* (1998), paper CFF3, p. 519.
5. C. Dorrer, E. M. Kosik and I. A. Walmsley, *Opt. Lett.* **27** (2002) 548.
6. C. Dorrer, E. M. Kosik and I. A. Walmsley, *Appl. Phys. B-Lasers. O.* **74**(Suppl) (2002) S209.
7. S. R. Friberg and P. W. Smith, *IEEE J. Quantum Elect.* **23** (1987) 2089.
8. L. Sarger, P. Segonds, L. Canioni, F. Adamietz, A. Ducasse, C. Duchesne, E. Fargin, R. Olazcuaga and G. Leflem, *J. Opt. Soc. Am.* **B11** (1994) 995.
9. S. Rivet, M. O. Martin, L. Canioni and L. Sarger, *Opt. Commun.* **181** (2000) 425.
10. C. Iaconis and I. A. Walmsley, *Opt. Lett.* **23** (1998) 792.
11. Schott Optical Glass Inc. Optical glass. Technical report, The Company, Duryea, Pa., 1980.
12. G. P. Agrawal, *Nonlinear Fiber Optics*, 2nd edn. (Academic Press, San Diego, 1995).
13. R. W. Boyd, *Nonlinear Optics*, 2nd edn. (Academic Press, Amsterdam, 2003).
14. S. Smolorz and F. Wise, *Opt. Lett.* **23** (1998) 1381.
15. S. Smolorz and F. Wise, *J. Opt. Soc. Am.* **B17** (2000) 1636.
16. R. H. Stolen, J. P. Gordon, W. J. Tomlinson and H. A. Haus, *J. Opt. Soc. Am.* **B6** (1989) 1159.
17. K. Ekvall, C. Lundevall and P. van der Meulen, *Opt. Lett.* **26** (2001) 896.